Journal of Power Sources 247 (2014) 527–533

Contents lists available at ScienceDirect

Journal of Power Sources

journal homepage: www.elsevier.com/locate/jpowsour

A study of lithium ion batteries cycle aging by thermodynamics techniques

Kenza Maher [b], Rachid Yazami [a,b,*]

[a] Nanyang Technological University, School of Materials Science and Engineering and Energy Research Institute at Nanyang (ERIAN), Research Techno Plaza, X-Frontier Blk, 50 Nanyang Drive, Singapore 637553, Singapore
[b] TUM CREATE, 1 Create Way, #10-02 Create Tower, Singapore 138602, Singapore

ARTICLE INFO

Article history:
Received 13 May 2013
Received in revised form
6 July 2013
Accepted 16 August 2013
Available online 28 August 2013

Keywords:
Thermodynamics
Entropy
Enthalpy
Lithium ion batteries
Cycle aging
Phase transition

ABSTRACT

Lithium ion batteries (LiB) are cycled under a galvanostatic regime (~C/2-rate) between 2.75 V and 4.2 V for up to 1000 cycles. After each completed 100 cycles, the discharge capacity, capacity loss, average discharge potential were determined under the same C/2 rate. Then cells undergo an additional charge and discharge cycle at C/6 rate followed by a thermodynamics measurements test. This enables open-circuit potential (OCP), entropy (ΔS) and enthalpy (ΔH) data to be assessed.

It is found that with increasing cycle number, the entropy and enthalpy profiles show more significant changes than those observed in the discharge and the OCP curves especially at particular SOC and OCP values. These differences are attributed to the higher sensitivity of entropy and enthalpy state functions to changes in the crystal structure of the graphite anode and the lithiated cobalt oxide (LCO) induced by cycle aging compared to the free energy ΔG (OCP) alone. The thermodynamics data are supported by post-mortem X-ray diffractometry (XRD) and Raman scattering (RS) analyses on the electrode materials. The results show important LCO crystal structure degradation, whereas, surprisingly, the graphite anode remains almost unaffected by heavy cycling, if not improved.

1. Introduction

It is common knowledge that rechargeable batteries in general and LiB in particular will experience a natural decrease in energy storage performance upon extended cycling [1–8]. The main parameters controlling battery performance decaying with cycle number, N are: 1) depth of discharge (DOD) [1,9,10], 2) depth of charge (DOC) [10,11], 3) rates of charge and discharge [12–14], 4) temperature [15–19], 5) over-charge [20–22], and 6) over-discharge [19]. Performance decay with N includes decreased discharge capacity and average discharge potential [1,10,12–14], decreased power output [5,17,23] and increased internal resistances [12,24–26]. Performance decay originates from degradation of electrode and electrolyte materials upon aging and occasionally from losses in electrical contacts between active materials in the anode, cathode and current collector [27].

In this study LiB coin cells were cycled under constant charge and discharge rate of ~C/2 between 2.75 V and 4.2 V at ambient temperature in 100 cycle batches for up to 1000 cycles. After each 100 cycles, the cells underwent an additional charge and discharge cycle under C/6-rate enabling discharge capacity ($q_d(N)$) and average discharge potential ($<e_d(N)>$) to be assessed. Then a thermodynamics measurements test on the cells was run following which entropy and enthalpy data were collected and plotted vs. SOC and OCP.

We found well defined SOC and OCP areas where entropy and enthalpy data show significant changes compared with barely detectable changes in the corresponding discharge and OCP profiles. Differences in data resolution between entropy and enthalpy on one hand and OCP on the other hand are attributed to amplified changes in thermodynamics characteristics of anode and cathode with cycle aging at particular SOC and OCP values where phase transitions and phase conversion takes place.

Post-mortem XRD and RS analyses performed on anode and cathode of a fresh cell and of a 1000 times cycled cell provide direct evidence for LCO crystal structure degradation and graphite structure resilience if not, surprisingly, enhancement.

* Corresponding author. Nanyang Technological University, School of Materials Science and Engineering and Energy Research Institute at Nanyang (ERIAN), Research Techno Plaza, X-Frontier Blk, 50 Nanyang Drive, Singapore 637553, Singapore.
E-mail address: rachid@ntu.edu.sg (R. Yazami).

0378-7753/$ – see front matter © 2013 Elsevier B.V. All rights reserved.
http://dx.doi.org/10.1016/j.jpowsour.2013.08.053

2. Experimental

2.1. Cycling condition and capacity loss determination

LiB coin-cells (2032, rated ~44 mAh) are used in this study. Cells were cycled between 2.75 V and 4.2 V under 20 mA constant current (~C/2-rate) at the ambient temperatures using an Arbin Instruments Battery Cycler. After each completed 100 cycles, the cells discharge capacity, capacity loss, average discharge potential and energy under the same C/2-rate were determined.

2.2. Thermodynamics measurements and state of charge determination

After each finished 100 cycles cells are transferred to the Electrochemical Thermodynamics Measurement System instrument (ETMS, Battery Analyzer BA-1000®, KVI PTE LTD, Singapore) to run following sub-steps:

a Conditioning cycle: Cells are charged to 4.2 V under C/6 rate then a constant 4.2 V was applied until the current dropped below 0.05 mA (~C/900). Cells were then discharged to 2.75 V under C/6-rate and a constant 2.75 V voltage was held until current drops again below 0.05 mA. In this cycle the ETMS determines the cells' charge and discharge capacity. The later is used to determine the SOC during the next step.

b Electrochemical Thermodynamics Measurements (ETM) test in which the cells are charged by 5% increments up to 4.2 V at C/6 rate where SOC = 100%. At each SOC the cells temperature T is decreased from the ambient temperature (~25 °C) to 10 °C by 5 °C steps and the cells' OCP is monitored. After the last temperature step at 10 °C is completed the temperature is left to rise to 25 °C then an additional 5% increment is applied to the SOC. This enables entropy and enthalpy to be determined according to Eqs. (1) and (2), respectively.

$$\Delta S(x) = F\left(\frac{\partial E_0(x,T)}{\partial T}\right)_{x,p} \quad (1)$$

$$\Delta H(x) = -F\left(E_0(x,T) + T\left(\frac{\partial E_0(x,T)}{\partial T}\right)_{x,p}\right) \quad (2)$$

where E_0 (x,T) is the OCP at temperature T, x = SOC, F = Faraday constant, p = pressure

The same cells were then cycled again for an additional 100 cycles until reaching 1000 cycles.

At the end of 1000 cycles, one cell out of four used in this study was discharged to 2.75 V and opened in a dry box filled with argon. The anode and cathode were then washed with DMC dried in vacuum, and mechanically separated from their respective copper and aluminum substrates. Electrode powders were analyzed by XRD (Bruker D8 Advance diffractometer) using CuK_α radiation in the angular range of 15°–90° (2θ) for cathode and 20°–90° (2θ) for anode with 0.02° 2θ-step, and by Raman scattering RS spectrometry, using Renishaw inVia Raman microscope in the backscattering geometry at room temperature. Excitation was carried out with the 514 nm radiation of an argon ion laser of 20 mW power.

3. Results and discussion

3.1. Discharge results

Fig. 1a and b shows the discharge profiles vs. discharge capacity q_d (mAh) and vs. normalized capacity (or state of discharge SOD), respectively. Fig. 2a and b shows both discharge capacity and average discharge voltage $<e_d>$ decreased with N, as one expects. Reported in Table 1 are the discharge characteristics data including $q_d(N)$, $<e_d(N)>$, discharge energy $E_d(N) = q_d(N) \times <q_d(N)>$ and capacity $q_{CL}(N)$ loss given by:

$$q_{CL}(N) = \frac{q_d(1) - q_d(N)}{q_d(1)} \times 100 \quad (3)$$

($q_d(1)$ = discharge capacity after 1 cycle). The $E_d(N)$ trace displayed in Fig. 2c varies almost linearly (R = 99.3%) with N according to:

$$E_d(N)(\text{mWh}) = 133.6 - 0.0527 \times N \quad (4)$$

$E_d(N)$ dropped by 22% and 39% after 500 and 1000 cycles, respectively corresponding to an average decrease rate of 0.094% per cycle.

The cells' OCP profiles vs. q_d and SOC are traced in Fig. 3a and b, respectively. Contrarily to the OCP vs. q_d profiles, which show significant variation with N, the OCP vs. SOC curves in Fig. 3b lay on top of each, except at 0% and 5% SOC values. The OCP vs. SOC results should relate to the fact that at each SOC (and at constant temperature and pressure), the cathode and the anode equilibrium potentials; $E_0^+(SOC,N)$ and $E_0^-(SOC,N)$ depend only on the lithium stoichiometry in the active fraction of cathode and anode. After each cycle the fraction of active anode and active cathode decreases. Because SOC normalizes the active part of anode and cathode to 100%, the OCP given in Eq. (5) will vary a little with N, which explains the superposition of the OCP vs. SOC curves.

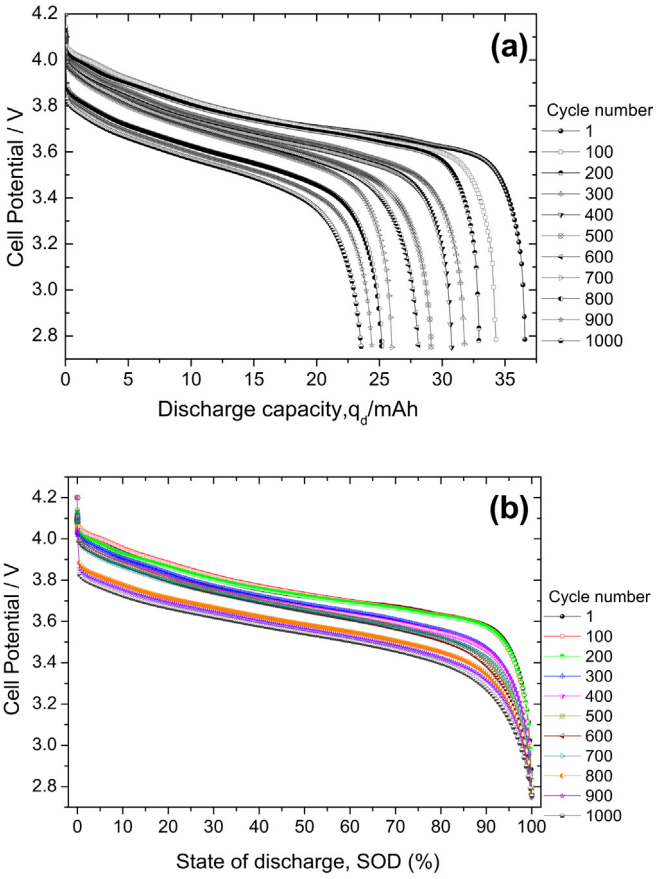

Fig. 1. Discharge profiles (C/2-rate) of LiB cells after cycling vs. discharge capacity (a) and vs. state of discharge (SOD).